Effect of New Turbine in a Gas-Liquid Mixing

Isao KONDO[1], Yoshikazu KATO[2*], Takahiro NEMOTO[2]

[1]*Tokyo Division, Satake Chemical MFG., Ltd.,
66 Niizo, Toda, Saitama 335-0021, Japan*
[2]*Mixing Laboratory, Satake Chemical MFG., Ltd.,
227-1 Niizo, Toda, Sitama 335-0021, Japan*

Keywords: Gas-Liquid Mixing, Mixing effect, Impeller, Disc Turbine

Abstract

Mixing blades possess the liquid fluidizing and shearing effects, both of which are combined to achieve agitation, and gas-liquid mixing is one of the systems which require these two conflicting effects. Disk Turbine type impellers with high shearing force, of which Rushton Turbine is probably the most famous brand, are typically used for gas-liquid mixing. Concave Turbine and Scaba have also been developed to cope with some shortcomings of Rushton Turbine, and fairly good research results of these impellers are being presented. However, we find no research reports have adopted a comprehensive and fundamental approach to the liquid fluidizing effect within an agitation tank, the fluidity of solid bodies, the dispersing effect and the shear failure effect during gas-solid-liquid mixing. Considering the function of conventional mixing blades, we believed it more important to alter basically the discharging effect of negative pressure generated at the rear side of a mixing blade and distinguish clearly one effect from another, particularly the liquid fluidizing effect exercised by the lift peculiar to a blade from the shear failure effect exercised by a strengthened shearing part near a pumping zone instead of trying to enhance liquid fluidization and shear failure simultaneously, when continuing our own research to improve the function for more effective stirring. As a result, we have succeeded in developing the sort of turbine that not only needs lower mixing efficiency but also improves bubble dispersion and liquid fluidization as well.

Introduction

The effects of a mixing blade are roughly classified into the 'liquid fluidizing effect' and the 'shear failure effect'. In order to adapt these effects appropriately to each purpose and process of stirring and obtain desired results, it is essential to study them separately based on systematic approaches.

This thesis relates to HS100 which, by analyzing the function of a blade in gas-liquid mixing, we have developed as a new type turbine utilizing liquid fluidization and shearing effects separately and efficiently unlike conventional disk turbines such as Rushton Turbine.

Rushton Turbine, generally classified as a turbine with high shearing force, has been used mainly for stirring that requires the shear failure effect and the interface travel rate increasing effect within not only a multiple phase such as gas-liquid and gas-solid-liquid phases but also a mixed phase such as a liquid-liquid phase.

In recent years, Scaba, Concave and other turbines have been manufactured to solve some problems of Rushton Turbine.

Rushton Turbine has its advantages of concentrated pumping as a result of both negative pressure at the rear sides of its blades and high shear force caused by a pressure gradient such as Edge Vortexes and Trailing Vortexes. On the other hand, this conventional turbine also has some disadvantages, for instance, that while very powerful with no gas flow, but it suddenly reduces power consumption a great deal as a reaction of the negative pressure, causing dispersion and liquid fluidization to deteriorate during gas flow. Even though its demerits became conspicuous soon after the beginning of its use, the turbine has been used for decades.

Concave Turbine was able to control the vortex separation from the rear sides of its blades (particularly the separation from the blades' leading edges), a defect of Rushton Turbine, and proved its excellent gassed power feature. However, Concave Turbine is slightly better than Rushton Turbine, since its liquid fluidization is insufficient and it uses negative pressure generated by the rear sides of its blades for discharging.

To sum up, conventional turbines pumping by using the negative pressure and inertia force of their blades' rear sides, and produce high shear force as a result of both velocity gradient or

relative velocity (change of pressure) and vortex zones with turbulent energy (trailing and edge vortexes). It has been gradually proved, however, that the actual shear failure force is closely connected with flow dynamics in and around a pumping zone. Therefore, when developing HS100, we separated the liquid fluidizing effect of mixing blades from the shear failure force of a strong pumping zone and adapted each mixing effect appropriately to the fluidization conditions. The concept of HS100 is completely different from that of a conventional disk turbine, in that the new type turbine controls the vortex separation from its rear sides to the maximum degree, concentrates flow using its lift and produces strong shear failure force as a result of the gradient and change of pressure at the pumping zone.

Fig. 1 shows Disk Turbine HS100 arranging at both its top and bottom the blades whose angles of attack are designed to control the separation, as compared to the typical conventional turbines.

1. Experimental Conditions and Apparatus

We conducted experiments using all-acrylic flat bottom cylinder stirring tanks. The tank diameters are 0.98m, 0.49m and 0.24m, their volumes $1.5m^3$, 200L and 20L, respectively. We used water as operating fluid, air as gas flow, the mixing efficiency measuring machine (SATAKE, ONO SS050 and ST800), PTV (Particle Tracking Velocimetry, SATAKE), 3D-Lagrange Analysis Device (SATAKE), CFD (Computational Fluid Dynamics, FLUENT), LDV (2D-Laser Doppler Velocimeter, KANOMAX IFA-655) and DO meter (IIJIMA ELECTRONICS) for analytical and experimental purposes, and compared the mixing efficiency and other properties of new and conventional turbines by analyzing flow dynamics, simulating numeric values and measuring velocity and gas absorption performance. Reynolds number Re for stirring was set to $>5 \times 10^4$ within the complete turbulence zone as a necessary condition of each experiment. By setting PTV number of two-dimensional, sectional meshes to 4,225, CFD number of meshes to around 1,200,000 (k-ε model) and LDV's number of samples at each velocity point to 3,000, we calculated power number Np by mixing efficiency measurement, pumping flow coefficient Nqd from multiple integral flow Qd of velocity based on LDV pumping velocity measurement, and the absorption velocity, which indicates gas absorption performance, from comprehensive volume absorption coefficient KLa standardizing the liquid concentration, based
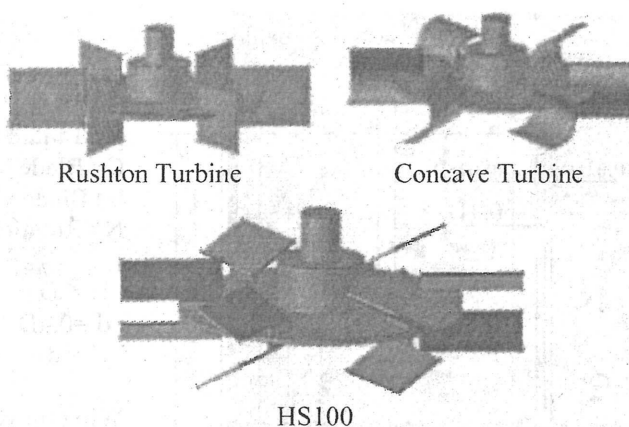

Rushton Turbine   Concave Turbine

HS100

Fig. 1 Comparison of new type and conventional disk turbines

Velocity and Flow analysis

Gas absorption performance measurement
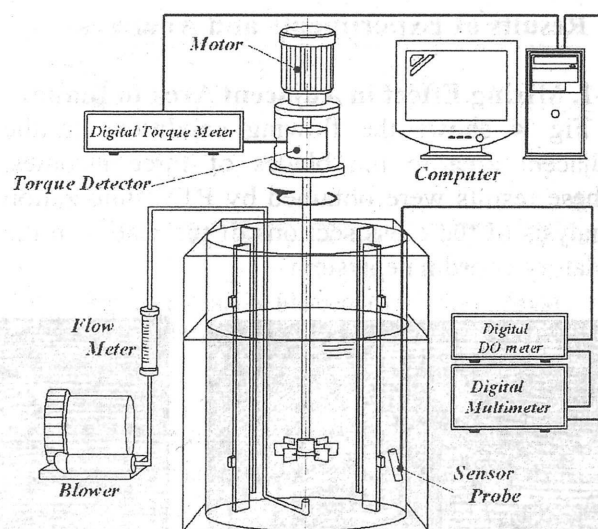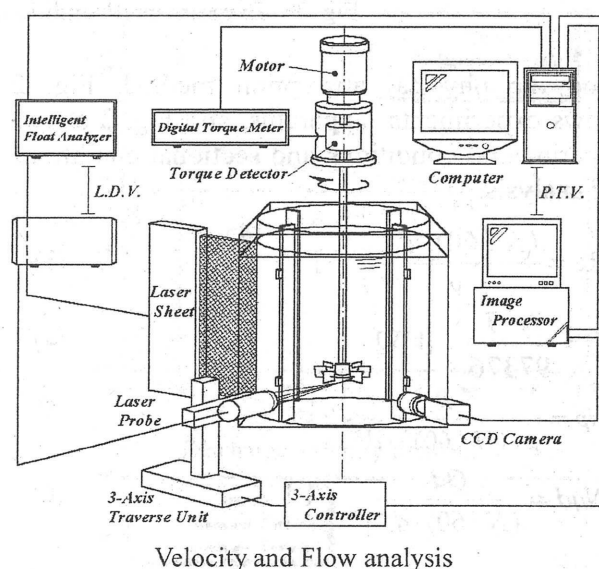
Fig.2 Experimental apparatus

$$KLa = \frac{1}{t} \ln \frac{C^* - C}{C} \quad [1/hr] \qquad (1)$$

D : Tank diameter   [m]
d : Blade diameter   [m]
H : Liquid height   [m]
C : Blade height   [m]
b : Blade width   [m]
N : Rotations   [min⁻¹]

$H = D$
$d = 0.4D$
$C = d$

Wing tip velocity:
$V_{tip} = \pi \cdot (N/60) \cdot d$ [m/s]   (2)

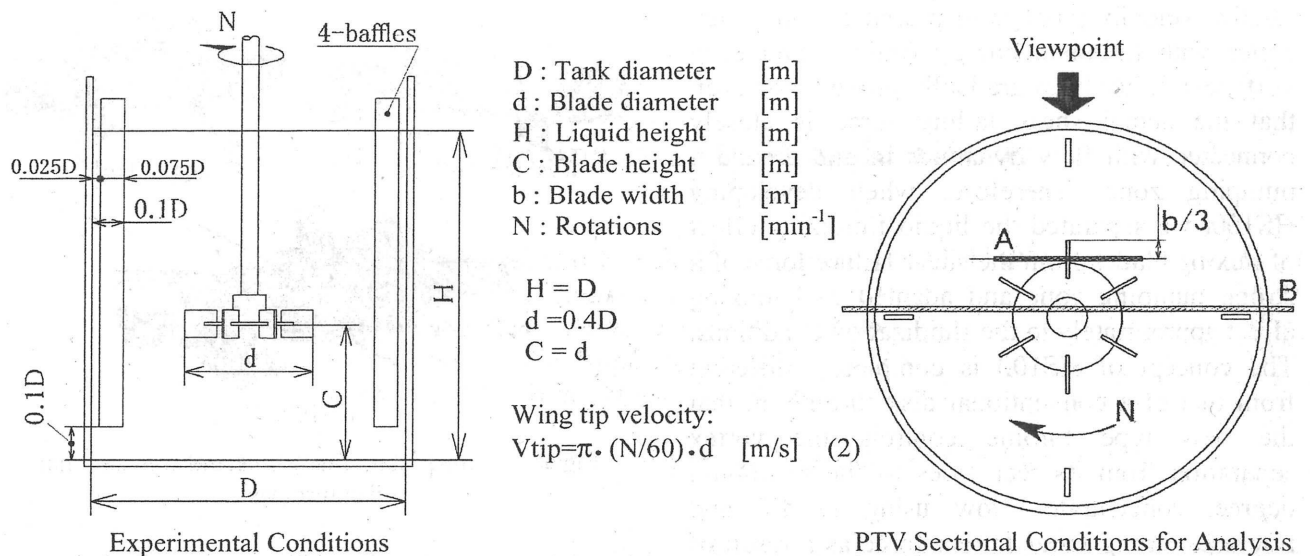Experimental Conditions   PTV Sectional Conditions for Analysis

Fig. 3   Experimental conditions and sectional conditions for analysis.

upon the physical absorption method. Fig. 2 shows experimental apparatus, and Fig. 3 shows experimental conditions and sectional conditions for analysis.

$$Re = \frac{(N/60) \cdot d^2}{\nu} \quad [-] \qquad (3)$$

$$P = \frac{N \cdot T}{97376} \quad [kW] \qquad (4)$$

$$Np = \frac{P}{\rho \cdot (N/60)^3 \cdot d^5} \quad [-] \qquad (5)$$

$$Nqd = \frac{Qd}{(N/60) \cdot d^3} \quad [-] \qquad (6)$$

2. Results of Experiments and Analyses

2-1. Mixing Effect in Adjacent Area to Blades

Fig. 4 shows the flowing conditions in the adjacent area to the blades of three turbines. These results were obtained by PTV fluidization analysis of the cross sections of the blades in the rotatory coordinate system.

Based on the analysis result of Rushton Turbine, it is possible to understand the quantitative feature of the turbine's negative pressure, that is, its edge vortex and flow into the rear side of its blade, and this feature pumping strong flow and high shearing force. When Rushton Turbine is stirring an actual zone with much gas flow, however, bubbles collect in the negative pressure space, thus decreasing its shearing force, pumping performance, dispersion and liquid fluidization.

Concave Turbine controls particularly the vortex separation from the blade's front edge, and its fluidization characteristics are different from those of Rushton Turbine. As a result, the turbine inhibits bubbles from gathering around the blades' rear sides, thus raising its stirring capacity even with much gas. It can be confirmed, however, that the separation occurs around the center of each blade and vortexes tend to travel deeper inside the center. Therefore, as far as the negative pressure pumping feature of blades' rear sides is concerned, Concave Turbine is almost the same as Rushton Turbine.
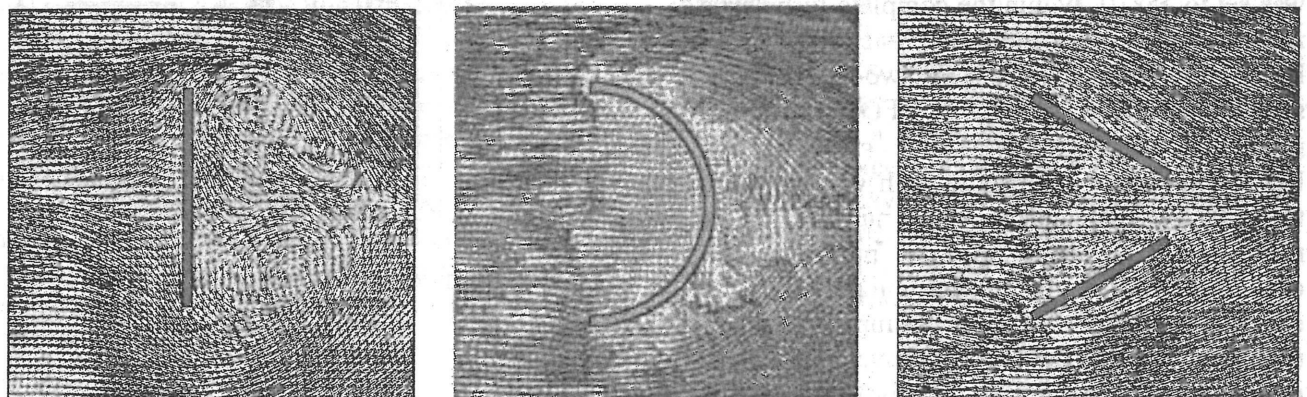
Rushton Turbine   Concave Turbine   HS100
Fig. 4   Results by PTV fluidization analysis of cross section A in the rotatory coordinate system $Re > 5 \times 10^4$

Vector on Blade Section A   Vector in Tank   Dynamic Pressure
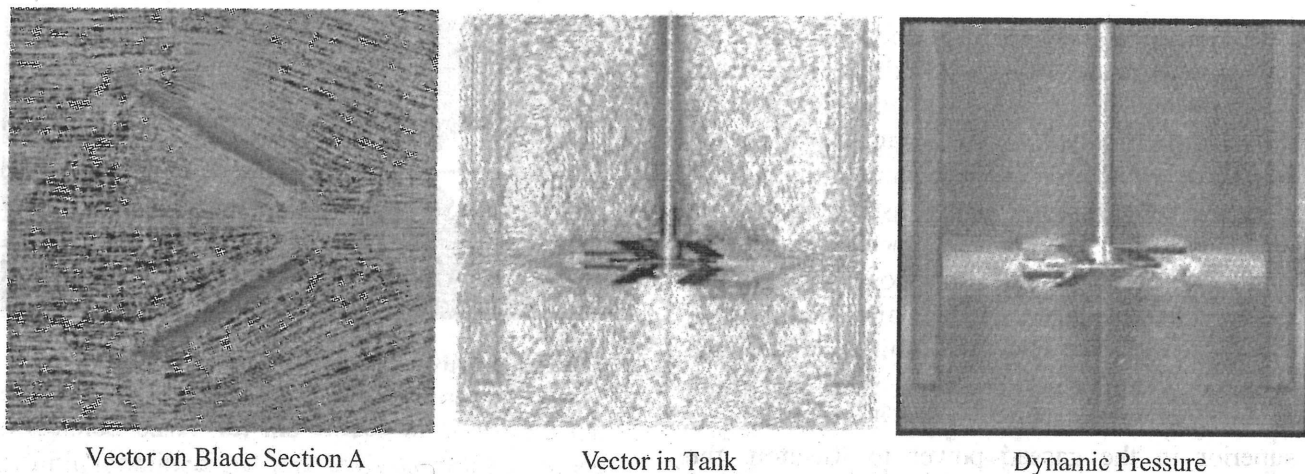
Fig. 5   CDF simulation results of HS100

The characteristics of HS100 are completely different from the conventional turbines. Firstly, vortexes never separate from the mixing blades arranged on the top and bottom of HS100. Secondly, the lift of each independent blade concentrates flow, thus forming the discharging source. Thirdly, as is clear from the analysis results, the HS100 has a fluidization capacity with no negative pressure space formed by vortex separation. This characteristics distinguishes HS100 from the conventional Disk Turbines. Fig. 5 shows the results of CFD simulation conducted under the same experimental conditions as above. The data of the fluidization feature, which are qualitatively identical, are now being used as supplementary tools for analytical purposes, but it is absolutely necessary to validate the data with actual phenomena.

Considering all the above results, it is evident that the mixing effect in the adjacent area to the blades of HS100 is different from those of the conventional turbines.

2-2. Pumping Feature

It is very important to understand not only the mixing effect in the adjacent area to blades but also the pumping feature as well. Fig. 6 shows pumping velocity characteristic curves obtained by LDV in order to compare the crucial pumping feature and its shear failure effect of the traditional turbines to those of HS100. Fig. 7 shows the analysis result by 3D Lagrange Analysis Device to compare the pumping and rotation velocity elements of the new type disk turbine to those of Rushton Turbine.

For these analyses, we used the stirring tank of which the diameter was 0.49m, and expressed the wing tip velocity leading edge as Vtip 2.5m/s, the radial (pumping) velocity element as Vd m/s and

Discharge Velocity Element

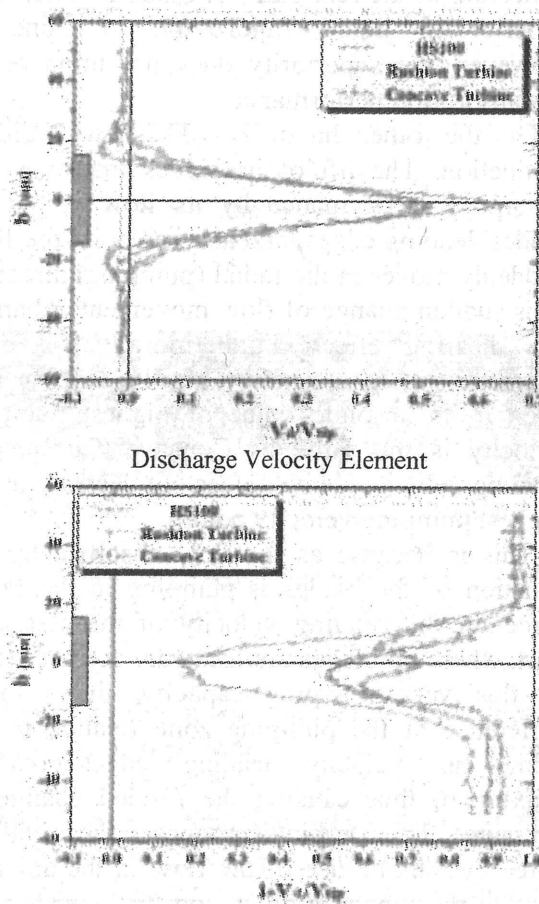Rotating Velocity Element (0 = Vtip=2.5m/s)
Fig. 6   Results of flow velocity measurement by LDV

the rotation velocity element as V θ m/s.

The comparison reveals that Rushton Turbine is characterized in its high pumping velocity, sharp distribution, steep velocity gradient and high rotating velocity. As a result, concerning the velocity vector of this disk turbine, the rotating velocity becomes maximum at the highest pumping velocity point, and therefore the velocity difference relative to the blade rotating speed, namely wing tip velocity Vtip leading edges is quite small.

The pumping feature of Concave Turbine is the same as that of Rushton Turbine, since even though the absolute values of both turbines are different their peaks are the same, that is to say the rotating velocity gets maximum at the highest pumping velocity point. Notwithstanding the fact that the power number of Concave Turbine is small and it is possible to boost its wing tip velocity leading edge under definite conditions of mixing efficiency Pv per unit volume, the absolute velocity of Rushton is higher than Concave. This is why, despite that Concave is superior in the gassed power to Rushton, the former is no better in the liquid fluidization effect than the latter. By restraining bubbles from collecting at the rear sides of blades, Concave is superior in liquid fluidization to Concave. However, the superiority does not improve its gas absorption performance.

On the other hand, HS100 shows evident distinction. The lift of its blades improves gas absorption performance by its flow up to the blades' leading edges, and at some point the flow suddenly moves in the radial (pumping) direction. This sudden change of flow movement enhances the shearing effect. Furthermore, it is most characteristic of the new type disk turbine that even if its absolute value of highest pumping velocity is the same as Concave Turbine the rotating velocity element does not decrease at the highest pumping velocity point

This is because as the flow absorbed by the function of the blades is pumping in the radial direction the rotating velocity of the clearance part, where no blades are located, decreases. Due to this very pumping capacity, the velocity difference at the pumping zone relative to the wing tip velocity leading edges reaches maximum, thus causing the sudden change of pressure. This turbine produces shear failure force by making use of the flow in the adjacent area to the pumping zone, and distinguishes the liquid fluidization effect completely from the shear fracture effect. In addition, the analysis results show the great value of turbulence of the pumping and rotating velocity elements at the time of pumping, which means that liquid fluidization in the stirring tank is stabilized and that the space of turbulence is enlarged.
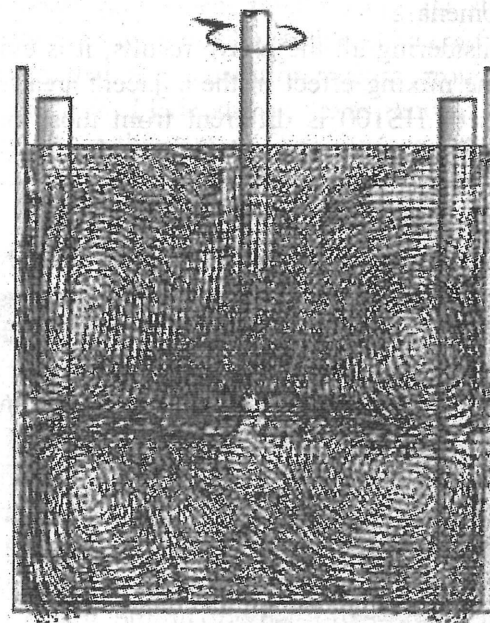
According to fluidization analysis results by 3D Lagrange Analysis Device shown in Fig. 7, the difference of relative velocity (synthetic velocity element) at the pumping zone between Rushton Turbine and HS100 can be confirmed visually, not quantitatively. Table 1 shows pumping flow rate coefficients Nqd, which were
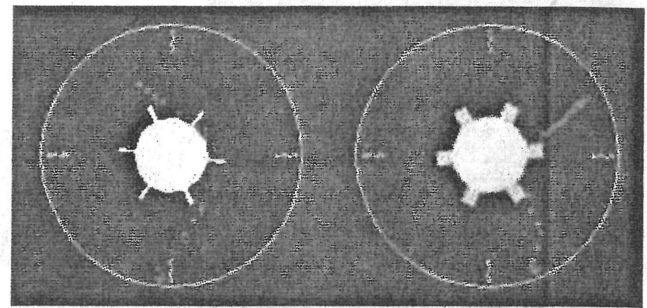
Rushton Turbine   HS100

Fig. 7   Comparison of discharge features by 3D Lagrange

Vtip
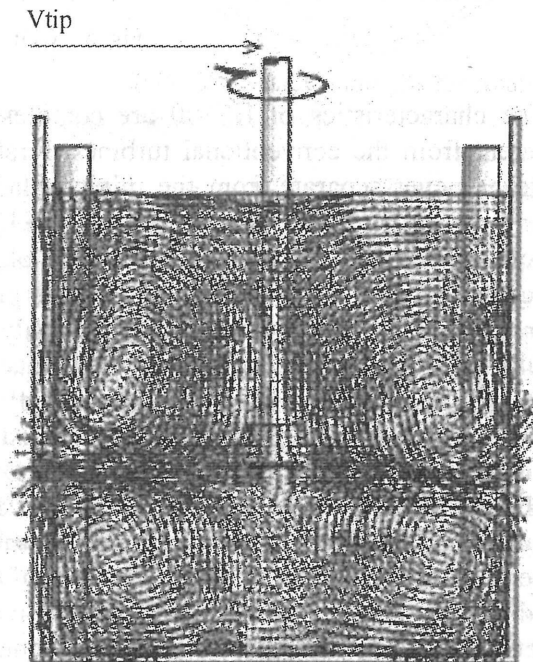
Rushton Turbin

HS100

Fig. 8   In-tank fluidization analysis results on section B by PTV

Table 1 Comparison of measured values and CDF results

Conditions	NP	Nqd
	HS100	
Measured Values	1.62	0.60
CFD	1.66	0.66

Np[-]: Power Number
Nqd[-]: Discharge Flow Rate Coefficient

calculated based on the values of flow rate Qd m³/min obtained by the analysis results. Since there are as much as 10% discrepancies between CDF simulation results and measured values, it calls for further validation.

2-3 In-Tank Fluidization Analysis Results

Fig. 8 shows PTV in-tank fluidization analysis results of Rushton Turbine and HS100. The stirring tank whose diameter was 0.24m was used, and the analysis results were expressed by vectors obtained by dividing local velocity V m/s by wing tip velocity Vtip m/s.

Concerning Rushton Turbine, its flow in the radial direction is fast, as is proved by LDV analysis, but four unique divided flow patterns, which do not reach the blades, appear right after discharging. These patterns cause the flow to slow down at both the top and particularly bottom of the tank. That is, since the flow is first absorbed into the strong negative pressure zone at the rear sides of blades and then pumping, fluidization within the whole tank is very difficult. In addition, the high rotating velocity element probably surpasses the small vertical velocity element in the tank, thus exacerbating fluidization.

On the other hand, regarding HS100, despite the fact that its velocity at the pumping zone is lower compared to Rushton, fluidization is much better both at the top and bottom of its tank. Unlike Rushton's flow patterns that cannot go for a long distance, HS100's circulating vortexes can be observed expanding up and down in the vertical direction. The new turbine produces excellent flow patterns not simply because the lift of blades absorbs flow from the whole tank but also because the rotating velocity element is small and the vertical velocity element is large. Whether flow patterns in the whole tank are good or bad depends very much upon the mixing effect in the vicinity of blades and the pumping capacity alike. When there is gas flow, the
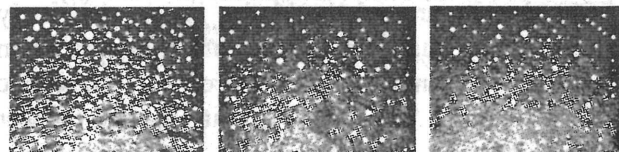
Table 2 Comparison of average bubble diameters

Rushton Turbine	Dp=2.56mm
Concave Turbine	Dp=1.93mm
HS100	Dp=1.81mm
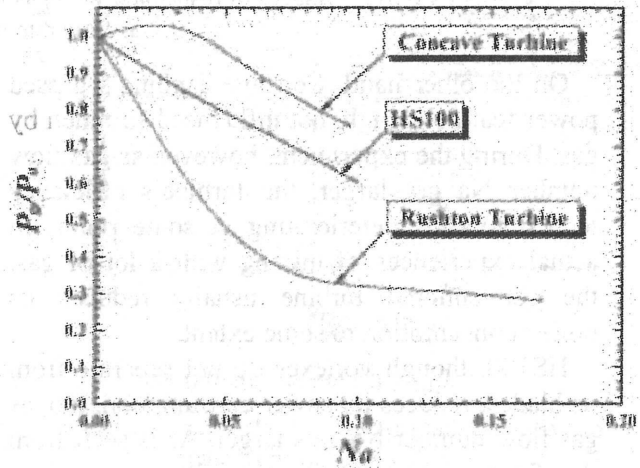
D=0.98 m, Vtip=5.0 m/s
Fig. 9 Gassed power feature

Rushton Turbine   Concave Turbine   HS100

Tank wall of discharge zone number of samples: 1,000
Fig. 10 Images of bubble diameters

difference in the mixing effect is even more obvious. The superiority of the new turbine contributes to the dispersion effect upon the air-liquid phase within the whole tank, to the solid dispersion effect upon the air-solid-liquid phase and to the heat conduction stirring method. CFD simulation results shown in Fig. 5 are not perfect reproductions of the flow patterns but qualitatively the same as actual fluidization analysis results.

2-4. Gassed power and Bubble Dispersion Features

Fig. 9 shows the comparison of each turbine's gassed power feature. We used the tank of which the diameter was 0.98m, and examined the analysis results from a variety of viewpoints.

As has been explained, power consumption of Rushton Turbine decreases very much simultaneously with gas flow.
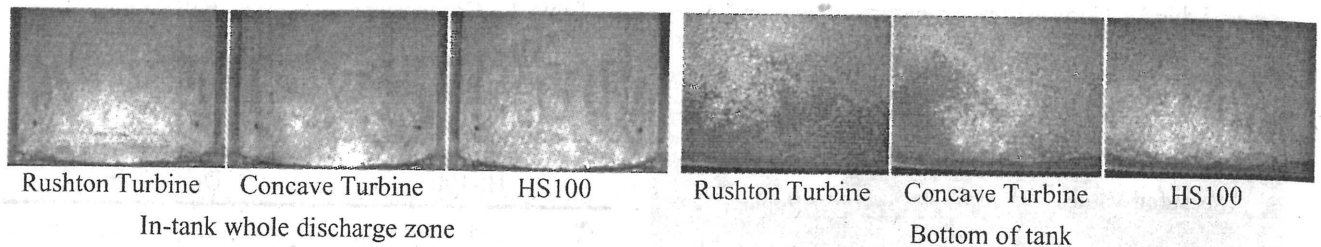
| Rushton Turbine | Concave Turbine | HS100 | | Rushton Turbine | Concave Turbine | HS100 |

In-tank whole discharge zone   Bottom of tank

Fig. 11   Images of dispersion with gas flow   Gassed power per volume Pgv=1.0kW/m^3
Gas flow rate per volume vvm=1.0

On the other hand, Concave Turbine's gassed power feature is high, not influenced so much by gas. During the experiment, however, as gas flow number Na got larger, the turbine's efficiency tended to start deteriorating at some point. In actual experiences of mixing with a lot of gas, the conventional turbine usually reduces its power consumption to some extent.

HS100, though vortexes do not separate from its blades, reduces its power consumption, too, as gas flow number Na gets larger. As is seen from the figure, however, its gassed power lowers linearly unlike the other traditional turbines. The new turbine might not be able to prevent all bubbles from twining the blades, but probably the density around the blades is just seemingly decreasing due to the improvement of dispersion capacity. Anyhow, we need to continue investigating the cause of its gassed power reduction.

Concave Turbine is thought to be excellent in its gassed power, but if HS100 is compared with Concave in terms of gassed power solely within the practical application zone of the line graph, the two turbine's capacity is almost the same.

Fig. 10 shows the images of bubble diameters on the tank wall of the pumping zone. The bubble diameters were obtained by binary processing of the photo images which were taken by emitting YAG laser on the tank walls and filtering. The number of sampling points was 1,000. Table 2 shows that the average bubble diameter by HS100 is the smallest, and that proves quantitatively the new turbine's dispersion performance is the most superb. However, it is important to find a better method of measurement for more accurate data. We need to clarify the difference of dispersion capacity of each turbine by using correct quantitative data and observing actual scenes of dispersion.

Fig. 11 shows the images of dispersion with gas flow. As for Rushton Turbine, bubbles do not spread to the bottom of the tank and hollow space is formed there, just as we proved the conventional turbine's feature in Section 2-3 In-Tank Fluidization Analysis Results.

Regarding Concave, bubbles do not disperse sufficiently at the bottom of the tank due to low pumping performance.

With respect to HS100, unlike the conventional disk turbines, since the location of the pumping zone is stabilized, bubble particles for upper and lower of the tank are observed spreading, and the bubble dispersion at the bottom of the tank is sufficient, either.

One of the most noticeable characteristics of HS100 is its lowered power, and it realized power number 1.62 during no gas flow, which is very small for a turbine (The power number of Rushton Turbine is about 5.0, and Concave around 2.5).

A low working power number makes it possible to heighten the blade diameter ratio and increase the number of rotations, thereby enhancing fluidization and dispersion all over inside a tank. Furthermore, a small power number enlarges the choice for blades, boosts the wing tip velocity leading edges and contributes to energy saving.

As is shown in Table 1, the power number obtained by CFD simulation is 1.66. The flow pattern of HS100 within a high Reynolds number range is qualitatively identical, while the power of the new turbine is quantitatively identical (the 2.5% discrepancy between the measured value and simulated value is negligible).

2-5 Comparison of Gas Absorption Performance

Fig. 12 shows the eventual influence for gas absorption performance by these efficiency that described above. This figure clarifies the transition of gas absorption capacity KLa relative to the change of gassed power per volume Pgv under the constant condition of standard in-tank ratio of gas flow rate per volume vvm=1.0 l/min.

The comparison reveals that gas absorption capacity KLa of HS100 is the highest, Concave Turbine comes second, and Rushton Turbine last. Fig. 13 compares Rushton Turbine with HS100 in terms of the transition of KLa relative to the change of gas flow rate under the definite

condition of gas flow late per volume vvm under the definite condition Pgv1.0kW/m³. The comparison shows again that the new type disk turbine is superior to other disk turbine.

Conclusion

It is not efficient, especially in the gas-liquid agitation, to provide the liquid fluidizing and shearing effects simultaneously in the form of pumping feature using negative pressure generated by the rear side of blades. The Disk Turbine is the most efficient impeller for stirring. A conventional turbine generally uses negative pressure of its mixing blades' rear sides for discharging and applies the liquid fluidization and shear failure effects simultaneously, but this method is not effective or efficient particularly for the stirring of an air-liquid phase. Conventional Disk Turbines have been used for a long period of time in spite of their obvious disadvantages. As the production system of many kinds and small quantity is getting prevalent, the purposes of stirring are likely to be more and more complicated and advanced, and conventional turbines will soon be at the limits of their capacity. It is important, therefore, to contrive better stirring methods by learning the characteristics of conventional turbines.

There exists abundance of literature, though we draw attention to the importance of understanding the characteristics and phenomena of disk turbines and mixing blades, distinguishing one essential effect from another, especially the liquid fluidization effect from the shear failure effect, and applying the right feature to the right stirring needs on your own, by making use of current state-of-the-art analytical technology.

We have provided herein the findings of HS100's superiority in high efficiency, namely, its lowered power, excellent fluidization and enhanced gas absorption performance by analyzing each different effect of this new type disc turbine systematically.

However, HS100 is not all-purpose and still has many problems for practical uses. For instance, where high pressure and high shear force are needed under the condition of no air flow, Rushton Turbine is still superior to the new turbine.

In conclusion, in order to provide the right stirrers and mixing blades for the right purposes in the future, we must examine crucial effects rationally from the viewpoint of fluids engineering and apply them separately and appropriately.
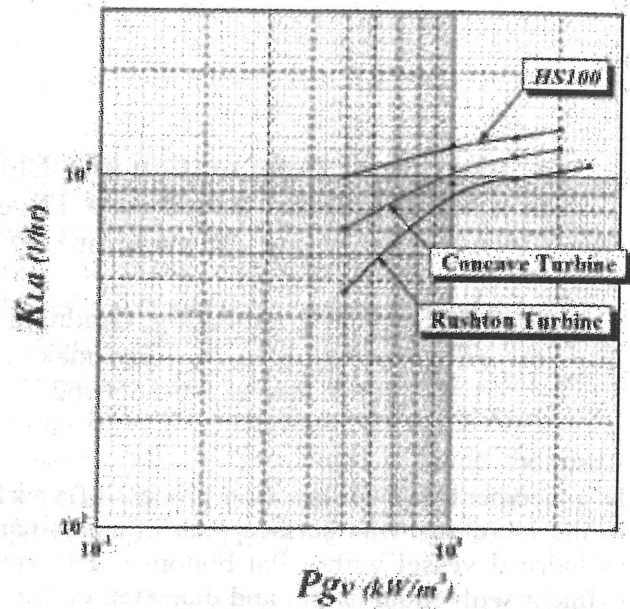
D=0.98m,   vvm=1.0 1/min

Fig. 12   Gas absorption performance relative to gassed power per volume
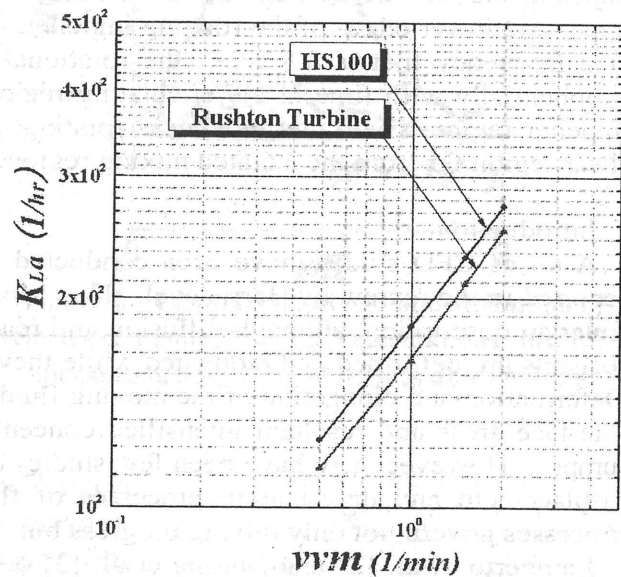
D=0.49m,   Pgv=1.0 kW/m³

Fig. 13   Gas absorption performance relative to gas flow rate per volume

$$Pv = \frac{P}{V} \quad [kW/m^3] \qquad (7)$$

$$Pgv = \frac{Pg}{V} \quad [kW/m^3] \qquad (8)$$

$$vvm = \frac{Qa}{V} \quad [1/min] \qquad (10)$$

$$Na = \frac{Qa}{N \cdot d^3} \quad [-] \qquad (11)$$

Mixing power : P[kW]
Gassed power per volume : Pgv [kW/m³]
Liquid volume: V [m³]
Gas flow rate: Qa [m³/min]